"Snowflake" divertor configuration in NSTX

V. A. Soukhanovskii, J. W. Ahn, R. E. Bell, D. A. Gates, S. Gerhardt, R. Kaita, E. Kolemen, H. W. Kugel, B. P. LeBlanc, R. Maingi, R. Maqueda, A. McLean, J. E. Menard, D. M. Mueller, S. F. Paul, R. Raman, A. L. Roquemore, D. D. Ryutov, H. A. Scott

June 7, 2010

Disclaimer

This document was prepared as an account of work sponsored by an agency of the United States government. Neither the United States government nor Lawrence Livermore National Security, LLC, nor any of their employees makes any warranty, expressed or implied, or assumes any legal liability or responsibility for the accuracy, completeness, or usefulness of any information, apparatus, product, or process disclosed, or represents that its use would not infringe privately owned rights. Reference herein to any specific commercial product, process, or service by trade name, trademark, manufacturer, or otherwise does not necessarily constitute or imply its endorsement, recommendation, or favoring by the United States government or Lawrence Livermore National Security, LLC. The views and opinions of authors expressed herein do not necessarily state or reflect those of the United States government or Lawrence Livermore National Security, LLC, and shall not be used for advertising or product endorsement purposes.

"Snowflake" divertor configuration in NSTX[☆]

V. A. Soukhanovskii[a,*], J.-W. Ahn[b], R. E. Bell[c], D. A. Gates[c], S. Gerhardt[c], R. Kaita[c], E. Kolemen[c], H. W. Kugel[c], B. P. LeBlanc[c], R. Maingi[b], R. Maqueda[d], A. McLean[b], J. E. Menard[c], D. M. Mueller[c], S. F. Paul[c], R. Raman[e], A. L. Roquemore[c], D. D. Ryutov[a], H. A. Scott[a]

[a]*Lawrence Livermore National Laboratory, Livermore, CA, USA*
[b]*Oak Ridge National Laboratory, Oak Ridge, TN, USA*
[c]*Princeton Plasma Physics Laboratory, Princeton, NJ, USA*
[d]*Nova Photonics, Inc., Princeton, NJ, USA*
[e]*University of Washington, Seattle, WA, USA*

Abstract

Steady-state handling of divertor heat flux is a critical issue for present and future conventional and spherical tokamaks with compact high power density divertors. A novel "snowflake" divertor (SFD) configuration that takes advantage of magnetic properties of a second-order poloidal null has been predicted to have a larger plasma-wetted area and a larger divertor volume, in comparison with a standard first-order poloidal X-point divertor configuration. The SFD was obtained in 0.8 MA, 4-6 MW NBI-heated H-mode discharges in NSTX using two divertor magnetic coils. The SFD led to a partial detachment of the outer strike point even in low-collisionality scrape-off layer plasma obtained with lithium coatings in NSTX. Significant divertor peak heat flux reduction and impurity screening have been achieved simultaneously with good core confinement and MHD properties.

1. Introduction

Divertor heat flux mitigation strategies presently envisaged for magnetically confined fusion plasma devices include both active techniques, e.g., gas-seeded radiative divertors, field ergodization and strike point sweeping, and passive techniques, e.g., divertor geometry and magnetic balance. These techniques aim at reducing the parallel heat flux $q_\parallel$ through volumetric loss processes in the SOL and divertor, partitioning of SOL power P_{SOL}, and reducing the heat flux $q_\perp$ deposited on the plasma facing components (PFCs) through increases in the plasma-wetted area [1, 2].

Additional challenges are anticipated for spherical tokamaks (ST). The ST is viewed as a candidate concept for future magnetic fusion and nuclear science plasma devices [3, 4]. In a low aspect ratio ST, its compact divertor geometry and the requirement of low core collisionality for adequate neutral beam current drive efficiency at electron densities $n_e \sim (0.5 - 0.7) \times n_G$ [3], where n_G is the Greenwald density, lead to a much reduced operational space of divertor heat flux mitigation schemes based on radiative and dissipative techniques. Experiments in the National Spherical Torus Experiment (NSTX) - a high-power density medium size ST ($R = 0.85$ m; $a = 0.65$ m) with graphite-tile plasma facing components (PFCs) - have already demonstrated the ST divertor challenges: ITER-level steady-state divertor heat fluxes $q_{pk} \leq 10 - 15$ MW/m^2 ($q_\parallel \leq 100$ MW/m^2) have been measured in $I_p = 1.0 - 1.2$ MA, 6 MW NBI-heated discharges [5, 6], making NSTX a good test platform for novel heat flux mitigation approaches.

In this paper we discuss initial results obtained with a novel "snowflake" divertor (SFD) configuration in NSTX. The SFD configuration [7, 8, 9, 10]

3

uses a second-order poloidal field null created by merging, or bringing close to each other, two first-order poloidal field null points (X-points) of a standard divertor configuration. The obtained hexagonal null-point magnetic equilibrium has an appearance of a snowflake. Poloidal magnetic field B_p in the vicinity of the second-order null increases with distance as r^2, as opposed to as r in the standard divertor (first order null) configuration. This leads to a lower B_p in the null region in the SFD, and as a result, higher poloidal flux expansion f_m, plasma wetted area A_{wet}, and a longer X-point connection length L_x, thus making a divertor volume available for radiation and momentum losses also higher [8, 10]. Magnetic equilibria with the SFD have been simulated for existing tokamaks [9], and in the TCV tokamak, the SFD configuration has been obtained using a set of six divertor coils [11]. In NSTX, the SFD configuration was obtained with two divertor coils in high-performance H-mode discharges. A salient feature of the SFD in NSTX was a partial detachment of the divertor outer strike point (SP) region with a significant reduction in divertor q_{pk} due to increased divertor radiation and momentum losses, and an associated significant reduction of core impurity density and radiated power.

2. Experiment

Magnetic control is critical for the SFD concept, since a second-order null configuration is topologically unstable [8, 10]. A predictive free-boundary axisymmetric Grad-Shafranov equilibrium code was used to simulate NSTX plasma equilibria with the SFD. The boundary shape and normalized pressure and current profiles from an existing high-δ discharge were used as in-

put. From the modeling, divertor coil currents and divertor strike point (SP) coordinates for the SFD were determined. In the experiment, the plasma control system (PCS) [12, 13] provided real-time control of SP positions by real-time variation of the PF1A and PF2L divertor coil currents (Fig. 1), using a proportional-integral-derivative (PID) controller algorithm with input from magnetic diagnostics. The SFD-like configurations with the outer strike point radius $R_{SP}^{outer} \simeq 0.55$ m were obtained in a number of discharges for periods of 50-150 ms using the PF2L coil for control (Fig. 1 (b)). The inner SP was held on the vertical target with $Z \simeq -1.55$ m using the PF1A coil for control. The SFD-like configuration was formed when the null-points separation d decreased below ~ 20 cm. Due to time-dependent plasma inductance l_i, ohmic transformer flux leakage, and variations in divertor structure eddy currents, the SFD-like configuration often intermittently changed to the standard divertor configuration. For example, the SFD discharge that will be discussed below in detail had six periods with the SFD-like configuration. To maintain the SFD for a whole discharge duration (1-2 s) we are presently implementing an additional lower divertor null-point real-time tracking and control capabilities in the NSTX PCS.

Magnetic and plasma characteristics of the SFD were studied in a $I_p = 0.8$ MA, $B_t = 0.4$ T discharge with 4-6 MW of NBI heating. These characteristics are compared to a similar medium triangularity $\delta \sim 0.65$ discharge with a standard divertor configuration (Fig. 1). In both discharges evaporated lithium coatings (80-100 mg per discharge) were used for wall conditioning and plasma performance improvements [14, 15]. Core and edge diagnostics used in this study have been described elsewhere [5, 16].

3. Results and discussion

The theoretically predicted magnetic geometry properties of the SFD [7, 8] were fully supported by reconstructions of magnetic equilibria with Grad-Shafranov equilibrium codes using standard magnetic and kinetic constrains [17]. In comparison with the standard divertor, f_m and A_{wet} in the SFD were higher by up to 90 %. The connection length L_x in the SFD was increased by up to 50 %. The divertor volume in the SFD available for volumetric losses was increased by 20-40 % . Divertor radial profiles of f_m and L_x showed that the second-order null-point affected the geometry in the first $2 - 3$ mm of the SOL (as mapped to the midplane) adjacent to the separatrix. Similar f_m and L_x were observed outside of this SOL region in both the standard divertor and the SFD.

Core plasma showed no degradation in H-mode confinement and performance in spite of the partial detachment in the SFD (Fig. 2). The lithium conditioning of these discharges resulted in the stabilization of low-n peeling-balooning edge modes and ELM suppression [18]. As with most of the NSTX discharges having suppressed ELMs, the standard divertor discharges showed impurity accumulation leading to $Z_{eff} \sim 2 - 4$ due to carbon and radiated power $P_{rad} = 1 - 2$ MW due to metallic impurities [19]. The core carbon inventory N_c and P_{rad} were reduced by up to 75 % in the discharges with the SFD as shown in Fig. 2 (c)-(d). While the detailed mechanism is yet to be confirmed, a reduction of divertor physical and chemical sputtering sources at low T_e during partially detached divertor operation was expected [20, 16, 5].

Divertor measurements during the SFD periods showed the commonly

observed characteristics of a partial SP detachment [1, 2, 5, 16]: an increase in divertor radiated power and momentum losses, a loss of parallel pressure balance, and as a result, a decrease of heat and particle fluxes to the plate. Shown in Fig. 3 are time traces of measured divertor characteristics. A good correlation was observed between the SFD periods indicated by $d \leq 20$ cm in Fig. 3 (a) on one hand, and increases in divertor D_α intensity induced by volume recombination (b), divertor neutral pressure increases (c), significant drops in the divertor heat flux averaged over the radial region $R = 0.45 - 0.60$ m (d), and divertor probe I_{sat} (e), on the other hand. While the heat flux measurements were uncalibrated due to lithium coatings on divertor surfaces, peak heat fluxes 4-6 MW/m^2 have been typical in similar no-lithium standard divertor discharges. A slow time response divertor bolometer signal showed a general 50 % increase in the SFD vs the standard divertor discharge (Fig. 3 (f)). A larger divertor radiating region of the SFD (in comparison with the standard divertor) was also evident in plasma visible camera images shown in Fig. 4 (a-b).

Divertor heat flux profiles measured at $t \sim 0.4$ s are compared in Fig. 4 (c). The heat flux values showed a 90 % reduction in a detached region of 2-3 mm (as mapped to the midplane) adjacent to the separatrix. In the attached SOL with $R_{div} \geq 0.6$ m, similar divertor heat fluxes were measured in the SFD and the standard divertor, due to similar magnetic geometries. Taking the SOL width $\lambda_{q_\parallel} \sim 6 - 7$ mm [6, 21] we conclude that a significant fraction of divertor heat flux was exhausted through volumetric processes in the SFD.

Divertor detachment is often accompanied by electron-ion recombination,

7

a process of volumetric ion momentum removal. The three-body recombination rate R is highly sensitive to local divertor plasma T_e, n_e due to $R \sim n_e^3$ and $R \sim T_e^{-4.5}$. The deuterium high-n Balmer series spectra are indicative of recombination rate R and local T_e, n_e, as their upper n-levels are populated by three-body recombination, the populations are governed by the Boltzman atomic level population distribution, and their Stark-broadening is due to electron and ion electric micro-field which becomes appreciable at high densities [22, 23]. In the SFD discharges, spatially resolved Balmer spectra showed a formation of a large volume recombination region, as indicated by the B10 line emission profiles in Fig. 4 (d). Note that in the medium-δ standard divertor case, the B10 emission originated predominantly in the PFR due to the UV spectrometer viewing the $R = 0.3 - 0.6$ region from above. The Balmer line intensities and shapes were modeled using the radiation transport and collisional-radiative code CRETIN [24]. The spectra were highly sensitive to both T_e and n_e, and the model implied that average $T_e \simeq 0.8 - 1.1$ eV and $n_e \simeq 2 - 7 \times 10^{20}$ m^{-3} were characteristic of the detached region in the SFD, as illustrated in Fig.4 (e). A comparison of the inferred electron pressure in the divertor region $p_e \sim (25 - 80)$ Pa to the midplane SOL pressure $p_e \sim (50 - 120)$ Pa measured in the SFD discharges showed that the pressure balance was generally not held.

The outer SP detachment does not occur in NSTX in standard divertor configurations at $P_{SOL} \sim 3$ MW because of insufficient divertor carbon P_{rad} [16]. Lithium conditioning tends to reduce recycling and divertor n_e thus making the detachment more difficult to achieve [25]. Owing to the SFD geometry properties, substantially increased volumetric losses led to a partial

8

detachment of the outer SP even at $P_{SOL} \simeq 3$ MW. Invoking the 1D model of electron conduction-dominated parallel heat transport with non-coronal carbon radiation as discussed in [16, 5], the measured increases in L_x and divertor n_e in the SFD would be sufficient to increase carbon P_{rad} and ion momentum losses necessary to reduce q_{div} to detachment. This is also in qualitative agreement with 2D multi-fluid modeling of the SFD for a DIII-D tokamak-like geometry [10].

In summary, the NSTX results provide support for the SFD concept as a promising divertor heat flux mitigation solution for next-step high-power fusion devices. We demonstrated that a SFD-like configuration could be generated with two divertor coils, and the SFD showed a higher plasma wetted area and a higher divertor volume in comparison with standard divertor configurations, as predicted theoretically. These geometry properties significantly increased the rates of divertor volumetric power and momentum losses, and led to reduced peak divertor heat flux, core impurities and radiated power while good H-mode confinement was maintained. New NSTX experiments are planned to study transport and turbulence in the SFD, dynamic divertor heat flux control via the SFD induced detachment, as well as the implementation of magnetic SFD control.

References

[1] ITER Physics Expert Group on Divertor et al., Nucl. Fusion **39** (1999) 2391.

[2] LIPSCHULTZ, B. et al., Nucl. Fusion **47** (2007) 1189.

[3] PENG, Y.-K. et al., Plasma Phys. Control. Fusion **47** (2005) 263.

[4] GOLDSTON, R. et al., in *Fusion Energy 2008 (Proc. 22nd Int. Conf. Geneva, 2008)*, CD-ROM file FT/P3-12, Vienna:IAEA, http:// www-naweb.iaea.org/napc/physics/FEC/FEC2008/html/index.htm.

[5] SOUKHANOVSKII, V. et al., Nucl. Fusion **49** (2009) 095025.

[6] GRAY, T. et al., Paper P2-65, These proceedings (2010).

[7] RYUTOV, D., Phys. Plasmas **14** (2007) 64502.

[8] RYUTOV, D. et al., Phys. Plasmas **15** (2008) 092501.

[9] RYUTOV, D. et al., in *Fusion Energy 2008 (Proc. 22nd Int. Conf. Geneva, 2008)*, CD-ROM file IC/P4-8, Vienna:IAEA, http:// www-naweb.iaea.org/napc/physics/FEC/FEC2008/html/index.htm.

[10] UMANSKY, M. et al., Nucl. Fusion **49** (2009) 075005.

[11] PIRAS, F. et al., Plasma Phys. Control. Fusion **51** (2009) 055009.

[12] FERRON, J. et al., Nucl. Fusion **38** (1998) 1055.

[13] GATES, D. et al., Nucl. Fusion **46** (2006) 17.

[14] KUGEL, H. W. et al., Phys. Plasmas **15** (2008) 056118.

[15] BELL, M. et al., Plasma Phys. Control. Fusion **51** (2009) 124054.

[16] SOUKHANOVSKII, V. A. et al., Phys. Plasmas **16** (2009) 022501.

[17] SABBAGH, S. et al., Nuclear Fusion **41** (2001) 1601.

[18] MAINGI, R. et al., Phys. Rev. Lett. **103** (2009) 075001.

[19] PAUL, S. et al., J. Nucl. Mater. **390-391** (2009) 211.

[20] WHYTE, D. et al., Nucl. Fusion **41** (2001) 1243.

[21] MAINGI, R. et al., J. Nucl. Mater. **363-365** (2007) 196.

[22] GRIEM, H. R., Phys. Scripta **T83** (1999) 142.

[23] WELCH, B. L. et al., Phys. Plasmas **2** (1995) 4246.

[24] SCOTT, H., J. Quant. Spectrosc. Radiat. Transf. **71** (2001) 689.

[25] SCOTTI, F. et al., Paper P3-6, These proceedings .
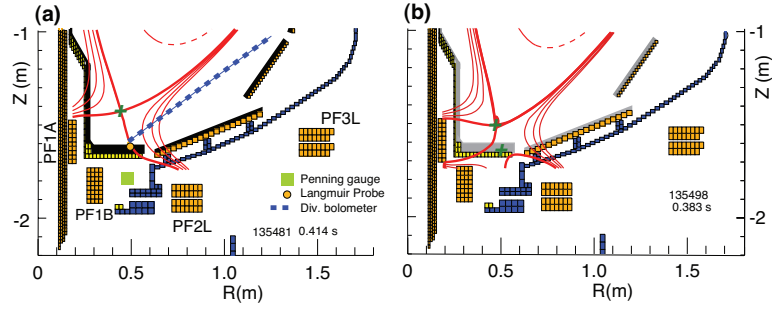
List of Figures

Figure 1: Medium $\delta \sim 0.65$ standard divertor (a) and SFD-like (b) configurations. Flux surfaces separated by 2 mm in the midplane are shown. Null points are indicated by crosses. Also shown are divertor Langmuir probe, neutral pressure Penning gauge, and divertor bolometer chord.
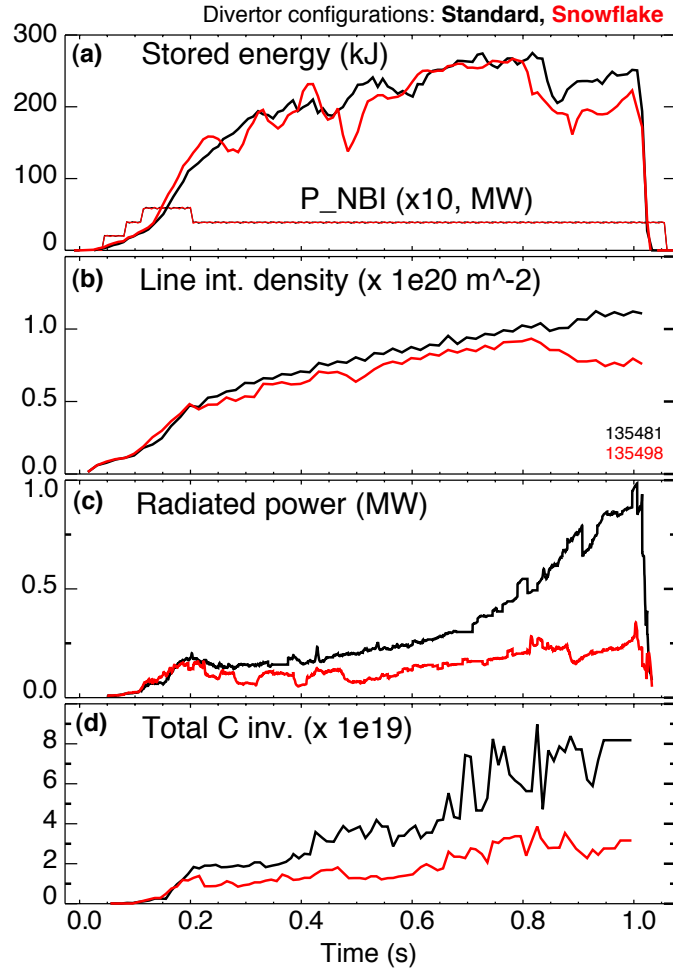
Figure 2: Time histories of core plasma quantities of the standard divertor and SFD discharges: (a) Stored energy W_{MHD} and P_{NBI}; (b) $\int n_e dl$; (c) Core P_{rad}; (d) Core carbon inventory.
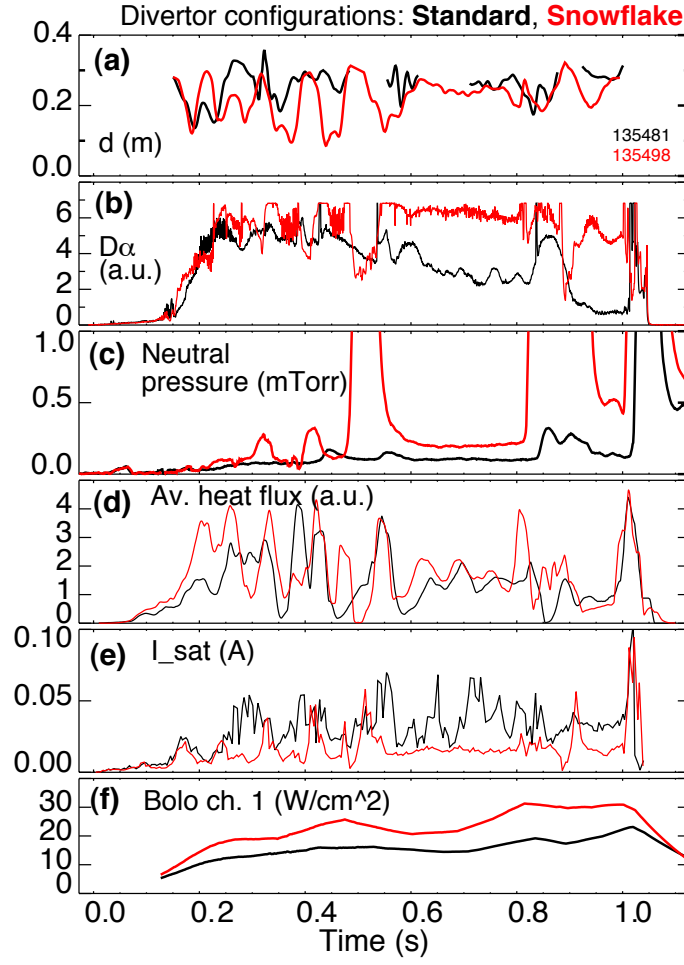
14

Figure 3: Time histories of divertor quantities of the standard divertor and SFD discharges: (a) null-point separation d; (b) Divertor D_α; (c) Divertor neutral pressure; (d) Average divertor heat flux; (e) Divertor probe I_{sat}; (f) Divertor bolometer signal.
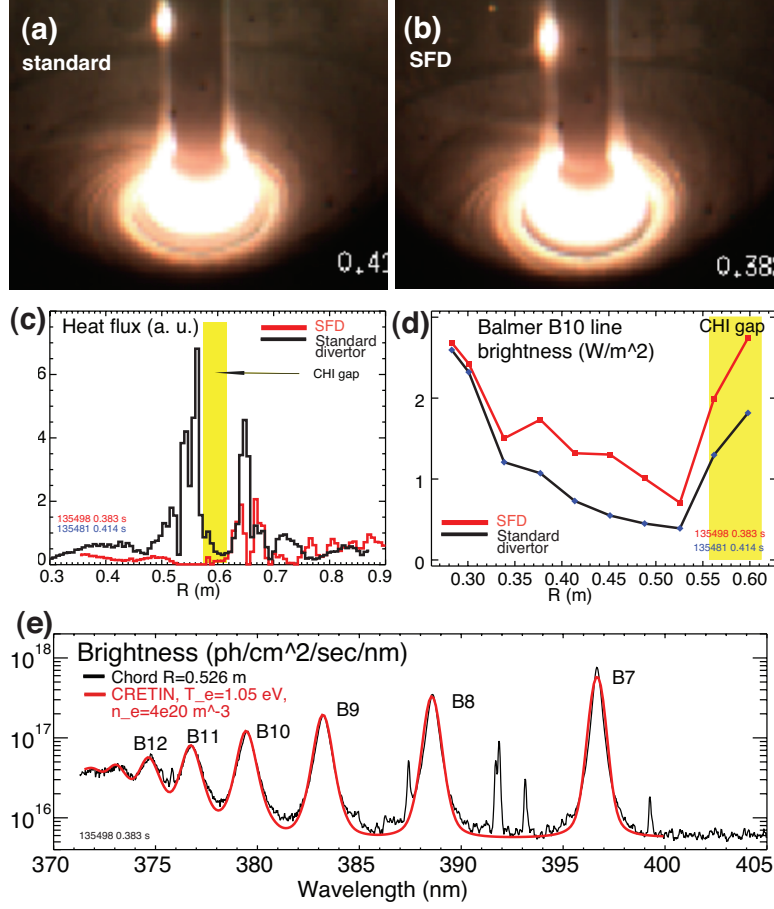
15

Figure 4: Divertor camera images of (a) standard divertor, (b) SFD. Divertor profiles (c) - heat flux, (d) Balmer B10 $\lambda = 379$ nm line brightness. (e) - Divertor Balmer spectrum measured at $R = 0.526$ m in the SFD and modeled with CRETIN code.

16